Effect of laminate thickness and of matrix resin on the impact of low fibre-volume, woven roving E-glass composites

L. S. Sutherland and C. Guedes Soares

Abstract

Instrumented falling weight tests led to the definition of three behaviour `regimes'; `undamaged', `internal delamination' and `severe' (at low, medium and high incident energies, respectively). The reduction in stiffness due to the internal delamination gave a bi-linear force–deflection relationship. A shear-dominated theory and an energy balance approach gave the relationship between incident energy and maximum force. By considering deviations from this model the complex impact behaviour seen was related to the damage modes observed. At low incident energies bending was significant for all except for the thickest polyester laminates. Delaminated behaviour was shear-dominated for all except the thinnest laminates. At higher incident energies back-face fibre damage controlled behaviour before membrane effects became significant for thinner laminates, and indentation damage of thicker laminates became influential. Subtle differences between the damage modes of the epoxy and polyester laminates were seen; the epoxy laminates suffered more back-face fibre damage, but less internal delamination.

Keywords

A. Fabrics, A. Glass fibres, A. PMCs, B. Impact behaviour

1. Introduction

Laminated fibre-reinforced composite materials are widely used in the marine industry due to their, good environmental resistance, the ease with which they may be formed into complex shapes, and also their high specific strength and stiffness. Composites are the dominant material for pleasure boat construction and are extensively used in the construction of fishing and naval vessels. High-speed craft such as fast ferries and patrol craft are now an increasingly important part of the marine industry, and the use of lightweight, corrosion resistant, readily fabricated and formed composites is ideal for such applications.

However, these materials are susceptible to out of plane impact. Impact damage may easily occur during construction, for example due to tool drops or during manoeuvring of components or modules. In-service impact events are also common, from often almost constant impact with waves, through frequent docking contacts, the striking of floating objects, collisions with other craft, to grounding.

The majority of the work in the area concerns high-cost aerospace materials, usually high fibre-fraction, pre-impregnated carbon-fibre epoxy based autoclave or vacuum-bag produced composites. Abrate [1] provides a comprehensive review and classification of the field. However, the composite materials used in the marine industry are generally much cheaper, low fibre-faction, hand laid-up, glass-reinforced, polyester or sometimes epoxy. There is very little available data concerning these `marine composites', and hence high safety factors and loss of potential weight savings are the norm. Mouritz et al. [2] quote safety factors of up to 10 applied when marine composite structures will be subjected to impact loads.

The analysis of the behaviour of an impacted laminate is usually split into two parts; the localised contact problem and the overall target deflection. Hertzian contact law is usually used to model indentation at the surface e.g., Sun et al. [3], Yang and Sun [4]). Complete models may be used to exactly describe the deformation of the target using beam or plate theories e.g., Chen and Sun [5] for simple cases of small deflections and simple material architectures. However, these models rapidly become too convoluted when considering more complex architectures, large deflections or cases with significant shear deformations. They are also not effective for the consideration of damage. In reality the response of a composite material to impact is complicated by numerous and interacting damage modes including internal delamination, surface micro-buckling, fibre fracture and matrix degradation [6]. The impact behaviour and the damage modes and paths are themselves dependant in a complex manner on the almost infinite material permutations including fibre and resin types, quantities, architectures, and interfaces, and also on the production method used [7–9]. Hence, especially for the inherently variable materials used in the marine industry, a more realistic approach in this case is to use theories to describe the overall response of the composite. The main available methods are the energy balance and spring-mass methods as described in [10], where a comprehensive overview of all of the main modelling techniques used may also be found.

The `impact response' of a composite material has proved difficult to standardise since the impact event itself is defined by many variables such as impactor and target geometries, impact speed and energy [11,12]. In order to approximate the most common type of impact seen in the marine industry, previous work [13] considered low-energy impact of low fibre-volume, woven roving E-glass composites. The transverse, central impact of a clamped plate with a small steel hemispherical impactor was considered as a relatively severe case.

An energy balance approach, assuming a bi-linear force–deflection relationship and that shear deflections dominated, gave the maximum force–incident energy relationship. Although correlation was seen, the model did not fit the thinner laminate data well since deflections due to bending were also thought to be influential. However, increasingly better agreement was seen as laminate thickness was increased. An aim of this work is to extrapolate the results of the previous work to thicker specimens to confirm the conclusions made about thicker laminate behaviour. Also in the previous work, two types of polyester resin were considered, orthophthalic (cheaper) and isophthalic (lower water absorption), but this was not seen to affect the impact response significantly. A further comparison is made here between the impact behaviour of polyester and epoxy resin composites.

2. Experimental details

The E-glass balanced woven roving reinforcement used was of 500 gm^{-2} with approximately 2.85 ends per cm (the `fine weave' version from the previous work). Panels of 5, 10, 15, 20 and 30 plies were laminated using orthophthalic polyester resin, and of 5, 10 and 15 plies using epoxy resin.

The same production method was used throughout. Cure of the polyester resin was achieved using 1% and 2% by mass of accelerator and catalyst, respectively, and 3% by mass of paraffin was also added to ensure full cure of the exposed panel surface. The epoxy resin was mixed with a slow hardener in the ratio of 5:1 by mass. One meter square flat panels were laid up by hand to achieve a fibre mass-fraction of 0.5 as representative of that

commonly achieved in the marine industry (equivalent to a fibre volume-fraction of approximately 0.35). 100 mm by 150 mm rectangular specimens, with the warp aligned with the longer dimension, were then cut from the laminated panels using a diamond-surrounded circular saw. Four thickness measurements were taken, one at each corner.

A Rosand instrumented falling weight impact (IFW5) test machine was used for the impact testing. The test specimens are pneumatically clamped between two steel `picture frames' of internal dimensions 120 mm by 75 mm, with the flat mould face of the specimen facing down. A 20 mm diameter steel impactor rod with a hemispherical end is connected to the bottom of a weight via a load cell. This is hauled to a prescribed height (corresponding to a prescribed incident energy) and then dropped down guide rails onto the specimen. Removable weights allow limited variation of the mass and hence the incident energy for a given velocity (or vice versa). As the impactor makes contact with the specimen an optical gate starts the data capture and measures the incident impact velocity. Software then calculates velocity, displacement and energy absorbed from the force–time data from the load cell.

Tests were performed at incident energy levels either up to perforation, or in the case of the thicker specimens up to the maximum value possible with the test machine. A mass of 10.853 kg was used for all tests, except for the lowest incident energy drop for each panel where a mass of 2.853 kg was used to give a feasible drop height. After testing, strong backlighting was used to measure the radius of the internal delamination for those tests where this was approximately circular.

3. Results

3.1. Polyester laminates

The damage seen may be divided into three distinct regimes corresponding to low, medium and high incident energies. At the lowest incident energies no damage was visible and the behaviour here may be categorised as `undamaged'. Load–displacement plots for these specimens were approximately linear, and the force–time plots approximately symmetrical (as an illustration of this low to medium incident energy 10-ply polyester results are shown in Fig. 1). However, the fact that there was hysterises in the load–displacement curve, and that approximately 70% of the incident energy was irreversible absorbed by the specimens indicates that some form of damage was present (Fig. 2).

At a very low threshold incident energy circular central internal delamination occurred. These delaminations then grew with increasing incident energy, and were accompanied by surface micro-buckling of the top ply rovings, indentation under the impactor, and matrix cracking on the back face. Here the load–displacement curves became bi-linear, with a drop in stiffness due to the internal delaminations, and the force–time plots became asymmetric (Fig. 1). The range of incident energies where this internal delamination is thought to dominate the behaviour is defined here as the `internal delamination regime'. This bi-linear behaviour was seen for all except the 5-ply specimens.

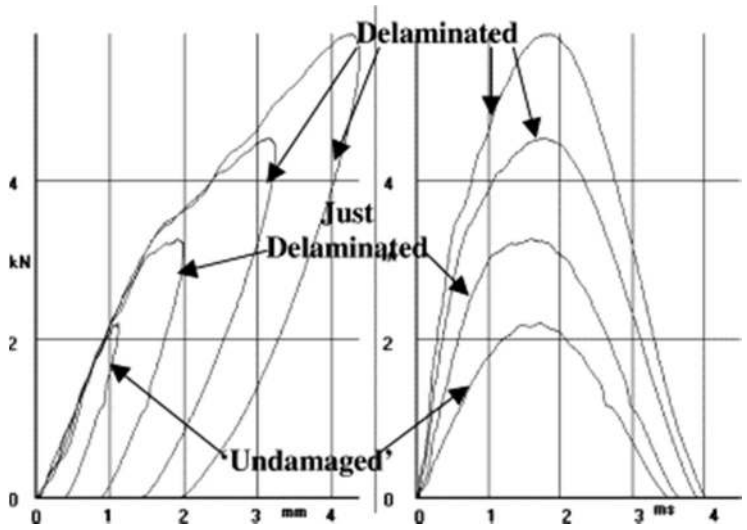

Fig. 1. `Undamaged' and `Delaminated' force–deflection and force–time plots.

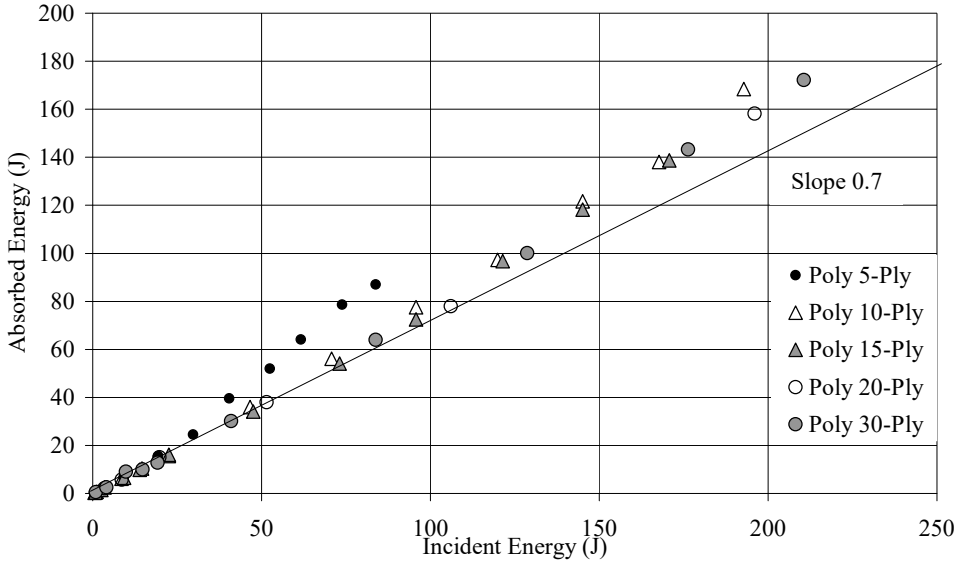

Fig. 2. Absorbed vs. incident energies polyester laminates.

As the incident energy was increased further, matrix degradation and fibre fracture occurred in an approximately circular region in the centre of the back face, and the top face and internal delaminations became rectangular or diamond shaped and then irregular. This damage then became progressively worse. For the thinner specimens, perforation or shear failure caused the final failure of the load bearing capacity of the specimen at the highest energies. This behaviour is defined as the `severe damage regime' and the effects of this fibre damage on the load–deflection and load–time plots can be seen in Fig. 3 (polyester 10-ply). The increased energy absorbed by this fibre damaged can be seen in Fig. 2 where the data diverges upwards from the linear relationship seen at lower incident energies.

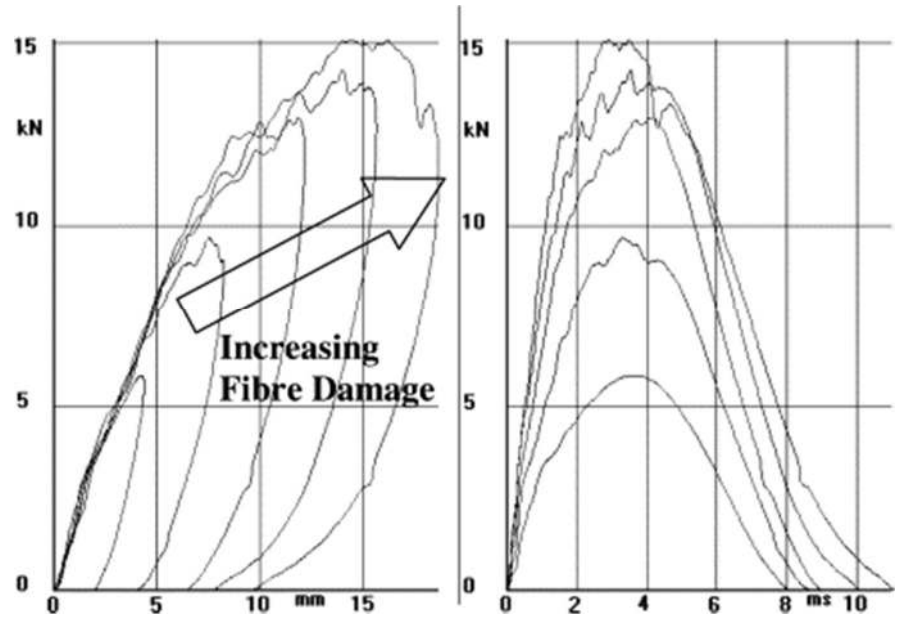

Fig. 3. Higher incident energy force–deflection and force–time plots.

With severe fibre damage the deflection continues to increase after the maximum load has been reached. In previous work [13] the difference between the deflection at the maximum load and the maximum deflection was used to quantify the onset of the severe damage regime, and the data for the polyester laminates is plotted in Fig. 4. However, this method can only be used to define the onset of severe fibre damage, it cannot accurately be used to show when back-face fibre damage first occurs or significantly affects the behaviour. Where fibre damage occurs the force–deflection and force–time plots in Fig. 3 become jagged, but force and deflection maximums may still occur almost simultaneously. The effects of this fibre damage are, however, visible in Fig. 4 for deflections of approximately 6 mm and above.

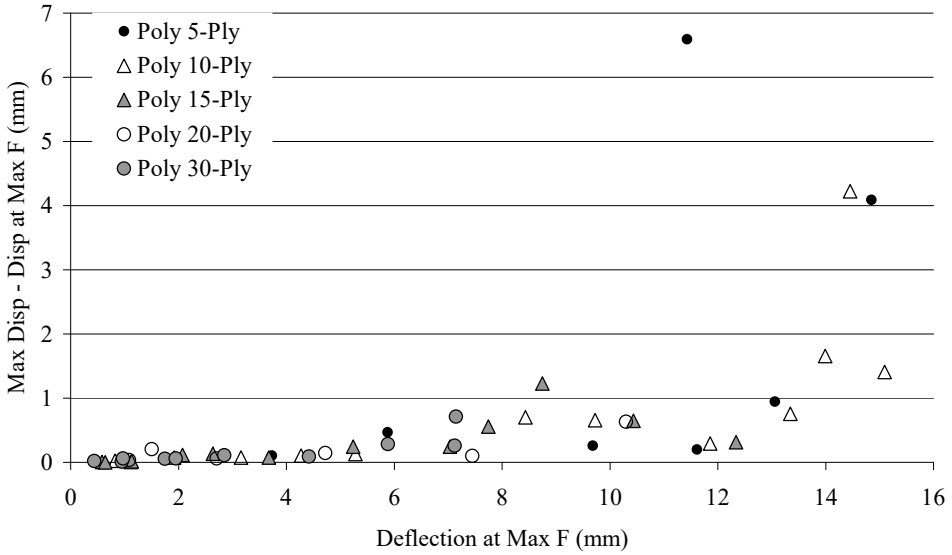

Fig. 4. Polyester specimens, onset of `Severe Damage Regime'.

The maximum incident energy attainable by the falling weight machine was not sufficient to produce significant back-face fibre damage in the thicker specimens, but especially for the 30-ply specimens, front-face indentation damage became important at higher energies.

Although little back-face damage was present, significant permanent indentation under the impactor occurred.

In Fig. 5 the circular internal delamination damage area is plotted against the incident energy. This area is the projected area of all internal delaminations; in some cases, especially for the thicker specimens, there was more than one internal delamination each at a different ply interface. The energy at which delamination was initiated increased with laminate thickness, but the shapes and slopes of the curves were similar for each laminate.

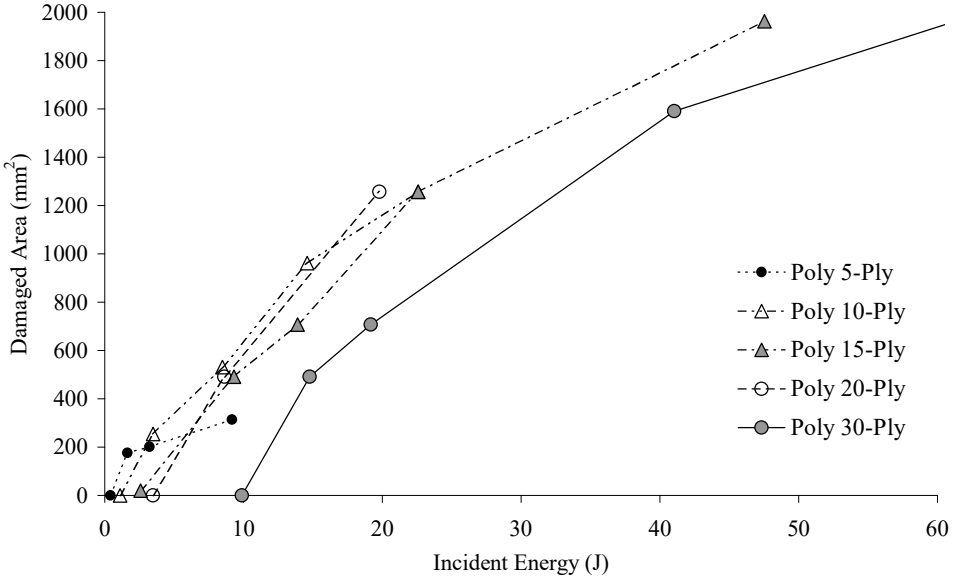

Fig. 5. Polyester laminates damage area vs. incident energy.

3.2. Epoxy laminates

Similar behaviour was seen for the epoxy specimens as shown in Figs. 1 and 2 for those of polyester. It was also pertinent to define the same three damage regimes for these laminates. However, there were differences in the damage modes obtained. Epoxy specimens suffered a greater area of front face delamination damage than equivalent polyester specimens impacted with equal incident energy. The internal delamination became lozenge shaped at relatively low energies. Back-face fibre damage was more severe for the epoxy specimens, occurred at lower energies and was of the form of a longitudinal line. The epoxy 5-ply force–deflection curve was bi-linear (unlike it is polyester equivalent), but, due to the jagged form of the second part, this was thought to be due to fibre damage and not internal delamination.

The absorbed energy vs. incident energy plot is very similar to that for the polyester tests (Fig. 6). There is some indication that for the 10- and 15-ply specimens the absorbed energy at low incident energies is slightly lower than that for their polyester counterparts. The points where the data deviates from the initial linear section for each laminate thickness are very similar to those seen in Fig. 2 for the polyester laminates (approximately 30, 70 and 100 J for the 5-, 10- and 15-ply specimens, respectively).

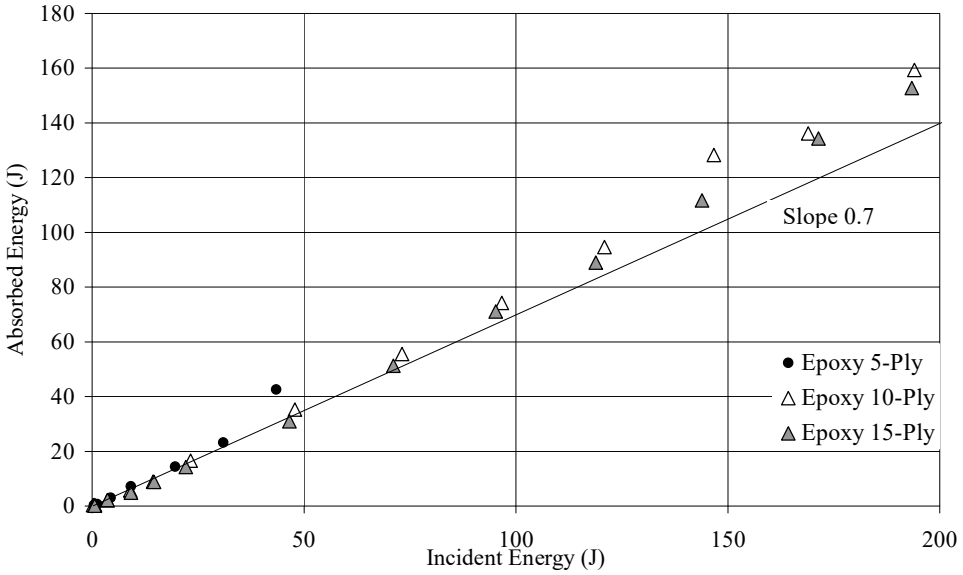

Fig. 6. Absorbed vs. incident energies epoxy laminates.

The effect of back-face fibre damage is again evident in Fig. 7 from about 6 or perhaps 5 mm. However, the shortcomings of the use of a cut-off value to define the severe damage regime are also evident. For example, the 5-ply tests gave complete perforation at higher energies, but due to the shape of the force–deflection plots, the difference between deflection at maximum force and maximum deflection were not large.

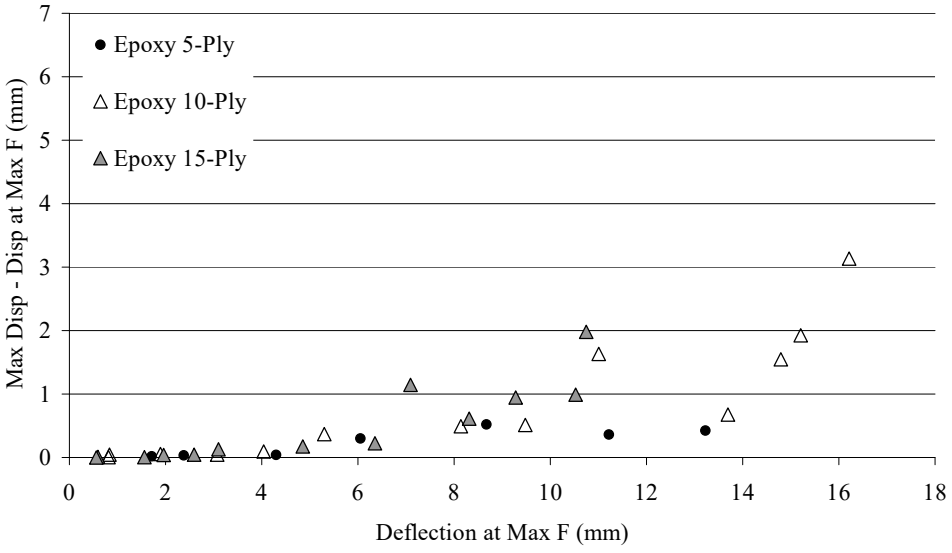

Fig. 7. Epoxy specimens onset of `Severe Damage Regime'.

Only circular delamination areas are plotted in Fig. 5. Comparison with Fig. 8 shows that the epoxy laminate internal damage becomes non-circular at much lower incident energies than does the polyester laminate damage. It is also evident that for equivalent incident energy for a given ply thickness the damaged area is much lower for the epoxy laminates. A very linear relationship is seen for the 15-ply results. Here there is no clear trend for the damage initiation energies with number of plies, although this could be because only a small number of data points are available around the initiation energy. For the same reason it is difficult to make accurate comparisons about the initiation energies with the polyester results.

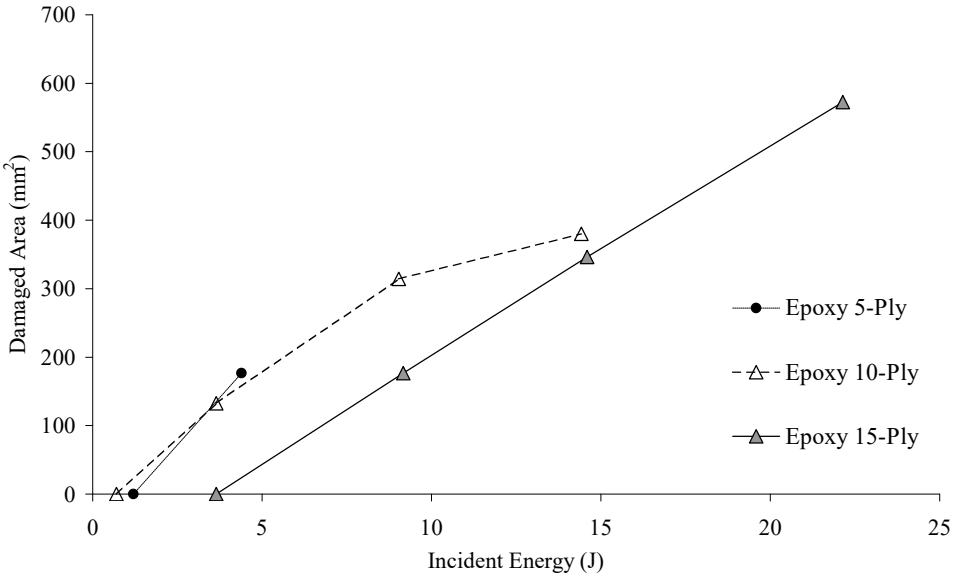

Fig. 8. Epoxy laminates damage area vs. incident energy.

4. Analysis and discussion

Only the data for those specimens that have not exhibited the final severe failure mode (defined here as those for which the difference between the maximum deflection and the deflection at the maximum force is less than 1 mm) is considered here. However, as will be seen, deviations from the theory due to fibre damage occur before this cut-off point.

Firstly the response of the laminate under the impact conditions is required in terms of force and deflection relationships. The force–deflection relationship may be written as [14]:

$$P = K_{bs} w + K_m w^3 \qquad (1)$$

where the effective stiffness due to bending and shear is given by

$$K_{bs} = \frac{K_b K_s}{K_b + K_s} \qquad (2)$$

The subscripts b, s and m for the stiffness *K* refer to bending, shear and membrane, respectively.

Shivakumar et al. also provide expressions for the stiffness of a circular, centrally loaded composite plate of the forms:

$$K_{bs} = \frac{K_b K_s}{K_b + K_s} \qquad (3)$$

where *h* is the plate thickness and A_0,B_0 and C_0 are terms involving only laminate material properties and plate radius. For a given composite material and plate diameter, A_0, B_0 and C_0 may be considered as constants.

Assuming that bending and/or shear deflections dominate (ie ignoring the membrane term in Eq. (1)), and combining Eqs. (1)–(3) gives:

$$P = C_o\left(\frac{h^3}{h^2 + C_o/B_o}\right)w \qquad i.e. \quad \frac{P}{h} = C_o\left(\frac{h^2}{h^2 + C_o/B_o}\right)w \tag{4}$$

Hence, a plot of force normalised by thickness vs. deflection should yield a linear relationship with a slope that increases with thickness asymptotically to a limit value of C_0. That is, for thick plates (or when the combination of material properties and plate diameter mean that shear deflections are much larger than those due to bending and hence $C_0 \ll B_0$) Eq. (4) reduces to:

$$\frac{P}{h} \approx C_o w \tag{5}$$

In this case, a plot of force normalised by thickness vs. deflection should yield a linear relationship that is independent of thickness.

It is assumed that for the low fibre volume fraction composites considered, which sustained considerable damage even at low incident energies, shear deflections generally dominate. The assumption is also made that the stiffness equations for rectangular plates have the same form as in Eq. (3). Eq. (5) may be modified to include the bi-linear force–deflection behaviour to cover both the `undamaged' and `delaminated' damage regimes.

$$\begin{array}{lll} \dfrac{P}{h} = C_0 w \qquad (a) & \qquad and \qquad & \dfrac{P}{h} = C_1 w + (C_0 - C_1)w_1 \quad (b) \\ for\ w \le w_1 & & for\ w \ge w_1 \end{array} \tag{6}$$

where (a) and (b) refer to the `undamaged' and `delaminated' behaviour, respectively, and w_1 is the deflection at delamination initiation. The values of C_0 and C_1 given in Table 1 are calculated as the relevant force–deflection plot slopes divided by the average laminate thickness. Here it must be noted that specimen thickness exhibits experimental variation due to the hand lay-up method used, with a coefficient of variation of approximately 0.05. Similarly, for a given laminate, the slightly different force–deflection slopes at different incident energies give another source of experimental variation.

Maximum force normalised by thickness is plotted against the deflection at the maximum force for the polyester and epoxy specimens in Figs. 9 and 10, respectively. The trend lines are plotted using the data from Table 1, the lines corresponding to thinnest and thickest laminates are closest to and furthest away from the *x*-axis, respectively. Considering the experimental scatter the data follows these trends well.

Firstly the polyester laminate results are considered. The slopes C_1 of the `delaminated' lines in Fig. 9 and Table 1 increase slightly with thickness for the thinner laminates, but approach a constant value for thicker specimens. This indicates that the behaviour is mostly shear dominated for the `delaminated regime', but that bending is significant for the thinnest laminates. The slopes C_0 of the `undamaged' specimens increase with thickness, but the 20- and 30-ply values are almost equal. This indicates that bending is significant for the `undamaged' regime, but that there is some evidence that shear deflection becomes dominant for the thickest specimens.

Laminate	Average Thickness (mm)	'Undamaged' Force-Deflection Slope (kN/mm)	C_O (kN/mm^2)	w_1 (mm)	'Delaminated' Force-Deflection Slope (kN/mm)	C_1 (kN/mm^2)
Polyester						
5-Ply	3.2	0.5	0.16	~	~	~
10-Ply	6.2	2.1	0.34	1.6	1.0	0.16
15-Ply	9.4	4.5	0.48	1.4	1.7	0.18
20-Ply	11.5	6.8	0.59	1.5	2.2	0.19
30-Ply	18.8	11.2	0.60	1.9	3.5	0.19
Epoxy						
5-Ply	3.3	0.5	0.16	~	~	~
10-Ply	6.0	2.2	0.37	1.9	1.0	0.17
15-Ply	9.1	4.9	0.54	1.9	2.1	0.23

Table 1. Bi-linear force–deflection behaviour data

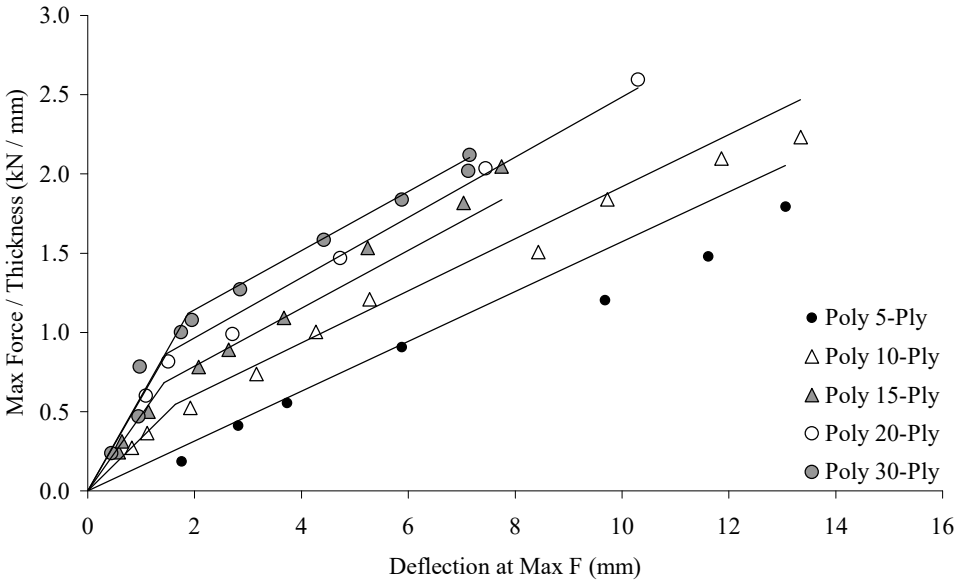

Fig. 9. Maximum force–deflection behaviour, polyester laminates.

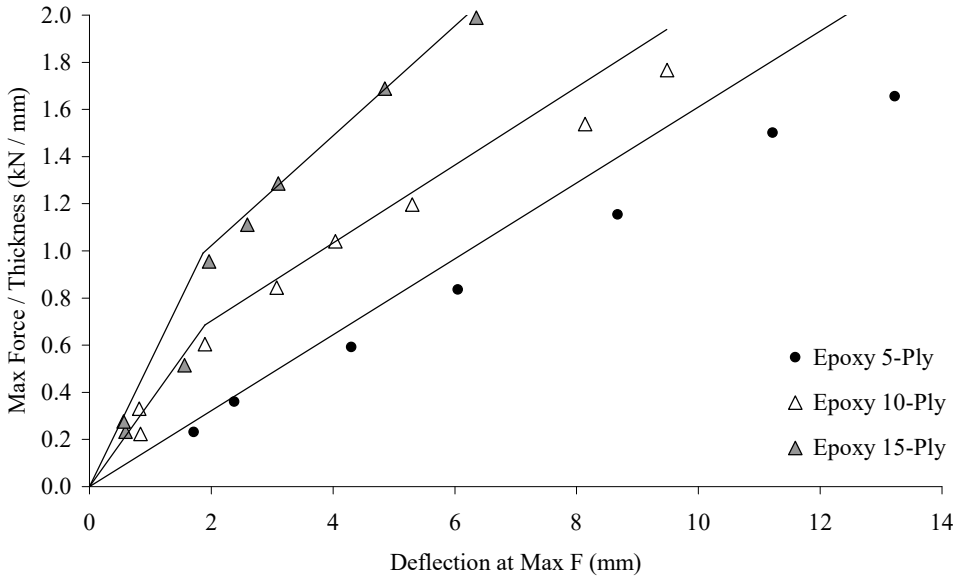

Fig. 10. Maximum force–deflection behaviour, epoxy laminates.

The data follows the trend lines fairly closely, but at higher incident energies deviations are seen. The complex interactions between many different failure modes at these higher energies means that it is not possible to explain with certainty this behaviour from the available data. However, the way in which the data has been presented here allows the proposal of probable explanations, with reference to observed damage modes, as discussed below.

The 5- and 10-ply data generally drops away from the trend line at higher deflections indicating that back-face fibre damage becomes important before the `severe damage regime' is defined. This also suggests that fibre damage becomes important before membrane effects can stiffen the behaviour at higher deflections. The fact that the crimp of the weave can straighten out (leading to damage) before membrane effects can take effect would explain this.

The 15-ply data shows a stiffening effect at higher deflections. This could be due to membrane effects, but this is unlikely given the discussion above. Another possible explanation is that of strain-rate effects; for a given laminate thickness, the impact duration is relatively constant whilst higher strains are reached at higher impact energies and deflections. Any strain-rate effect could be a property of the material, but in this case it is more probable that it would be linked to the rate of propagation of the internal lamination. Back-face fibre damage would be significant for the 5- and 10-ply laminates before any similar strain-rate effects become apparent.

The 20- and 30-ply data remain on the trend line at higher deflections. This could be because these thicker laminates were not subjected to sufficiently high incident energies to give deviations from the theory. Alternatively, since the higher loads experienced by these thicker specimens leads to more significant indentation damage, this front-face damage could offset any strain-rate effects.

Next the epoxy laminate results are considered. The `undamaged' behaviour shows a similar increase in C_0 with thickness as for the equivalent polyester laminates, but the initiation of delamination damage occurs at a higher deflection for the epoxy composite. The

`delaminated' behaviour shows a significant increase in C_1 with thickness, indicating that bending deflections are more significant here than for the equivalent polyester behaviour. Back-face fibre damage causes the data to fall off below the trend lines at higher deflections, generally becoming significant at lower deflections than for the polyester data. This increased back face-fibre damage would explain why no stiffening of the 15-ply epoxy response at higher incident energies is seen.

Now the force–incident energy relationships will be developed. In order to achieve this an energy balance approach is taken. It is assumed that all incident kinetic energy (IKE) is absorbed by the specimen as damage and potential energy (due to the specimen stiffness and deflection) when the maximum force is reached. Calculating the energy absorbed by integration of the force–deflection response, equating this to the IKE and normalising both sides by thickness gives:

$$\frac{IKE}{h} = \int_0^{w_{PMax}} \frac{P}{h}\, dw \qquad (7)$$

Substituting for P/h from Eq. (6) into Eq. (7) and integrating gives:

$$\frac{IKE}{h} = \frac{1}{2}\left(C_1 w_{PMax}^2 + 2(C_o - C_1) w_1 w_{PMax} + (C_1 - C_o) w_1^2\right) \qquad (8)$$

Rearranging Eq. (6) to give deflections in terms of force normalised by thickness and substituting into Eq. (8) gives the desired relationship between maximum force and incident energy;

$$\left(\frac{P_{Max}}{h}\right)^2 = 2C_o\left(\frac{IKE}{h}\right) \qquad (a)\ for\ IKE \le IKE_1$$

$$\left(\frac{P_{Max}}{h}\right)^2 = 2C_1\left(\frac{IKE}{h}\right) + \left(\frac{C_o - C_1}{C_o}\right)\left(\frac{P_1}{h}\right)^2 \qquad (b)\ for\ IKE \ge IKE_1 \qquad (9)$$

where IKE_1 and P_1 are the incident energy and force at which delamination first occurs. The polyester and epoxy composite data is presented in the form of Eq. (9) in Figs. 11 and 12, respectively. Again the lines corresponding to thinnest and thickest laminates are closest to and furthest away from the x-axis, respectively.

The data again follows the trend lines (constructed using the values in Table 1) well considering the experimental scatter. Almost identical behaviour as seen in Figs. 9 and 10, and discussed previously, is seen for higher energy impacts where the data deviates from the theory. This shows that the energy balance approach is very effective here in providing the relationship between the severity of the impact event and the maximum force.

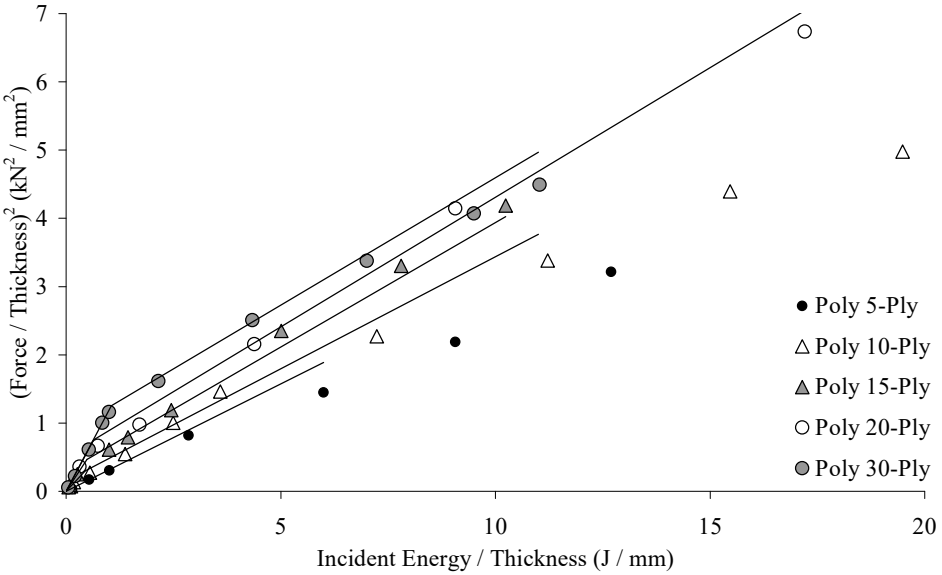

Fig. 11. Force–IKE relationship, polyester laminates.

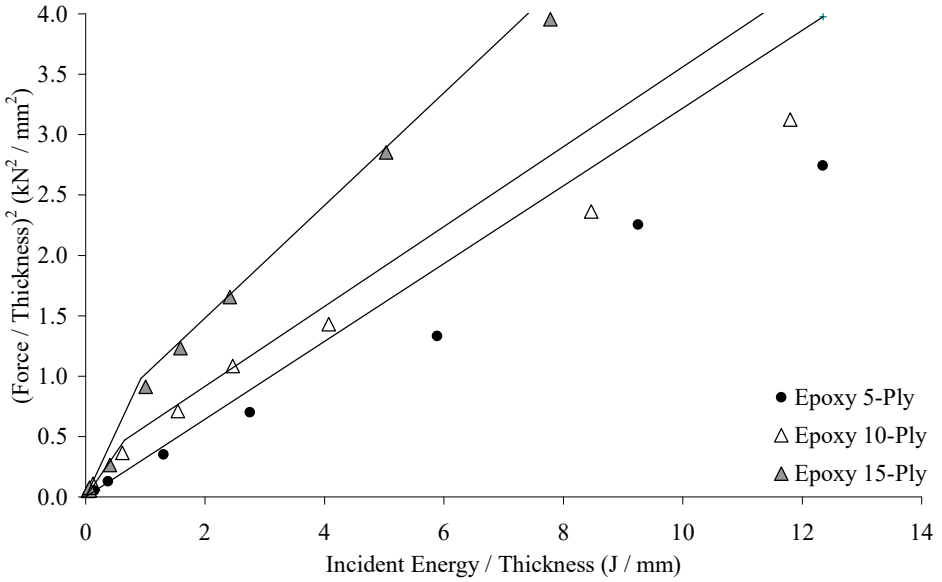

Fig. 12. Force–IKE relationship, epoxy laminates.

5. Conclusions

Instrumented falling weight impact tests on low fibre-fraction E-glass woven roving polyester and epoxy laminates have been performed. The behaviour seen has been classified into three regimes: `undamaged' (low incident energy, no visible damage), `internal delamination' (medium incident energy, internal delamination) and `severe' (high incident energy, back-face fibre damage). `Undamaged' behaviour was seen only at the very lowest incident energies and even here approximately 70% of the incident energy was irreversibly absorbed indicating some form of damage was in fact present. With the initiation of the internal delamination a reduction in stiffness produces a bi-linear force–deflection plot. The exact onset of the `severe' damage regime was difficult to define since, especially for the epoxy laminates, the effects of back-face fibre damage became significant gradually. For the thickest laminates indentation damage became important due to the lower deflections and hence higher contact loads seen.

The use of a bi-linear force–deflection theory together with an energy balance approach gave the relationship between the incident energy and the maximum force. Good agreement with the experimental data was obtained and the use of such a method enabled the nature of the behaviour to be identified. The results of the previous work have been extended to the behaviour of thicker specimens, confirming and clarifying the conclusions previously made. The thinner laminate response of both epoxy and polyester composites was significantly affected by bending deflections. At very low incident energies, the `undamaged' behaviour for all except the thickest polyester laminates was also significantly affected by bending deflections. The `delaminated' response of the polyester laminates was seen to be shear deflection dominated. However, bending deflections accounted for a significant part of the `delaminated' epoxy laminate response. Deviations from the theory at higher incident energies in the `delaminated' regime are thought to be due to fibre damage in the case of thinner laminates and indentation damage for thicker laminates. It is thought that further work to include the effects of indentation is necessary. A strain-rate effect, probably connected with delamination growth rate, was also perhaps active. The theory used does not apply to the `severe damage' regime seen at the highest incident energies.

Although broadly similar, subtle differences between the damage modes of the epoxy and polyester laminates were seen. The damage to the epoxy laminates was more elongated with more back-face fibre damage that occurred at lower incident energies than for the polyester laminates. The epoxy laminates also suffered more front-face delamination, but the internal delamination was smaller and was first seen at a higher incident energy. The method used enabled these differences in damage modes to be linked to the differences in impact behaviour seen. However the relationships between irreversibly absorbed energy (closely related to damage incurred) vs. incident energy were very similar for both laminates.

Acknowledgements

The first author has been financed by Fundação para Ciência e a Tecnologia, Lisbon, Portugal, under contract number SFRH/BPD/1568/2000.

References

[1] Abrate S. Impact on composite structures. Cambridge University Press, 1998.

[2] Mouritz AP, Gellert E, Burchill P and Challis K. Review of advanced composite structures for naval ships and submarines. Composite Structures 2001; 53: 21-41.

[3] Sun C.T., Dicken A., Wu H.F. Characterization of impact damage in ARALL laminates. Composite Science and Technology 1993; 49: 139-144.

[4] Yang S.H., Sun C.T. Indentation law for composite laminates. ASTM STP 787 1982:425-449.

[5] Chen J.K., Sun C.T. Dynamic large deflection response of composite laminate subject to impact. Composite Structures 1985; 4(1): 59-73.

[6] Richardson M.O.W. and Wisheart M.J. Review of low-velocity impact properties of composite materials. Composites Part A 1996; 27A: 1123-1131.

[7] Cartié D.D.R. and Irving P.E. Effect of resin and fibre properties on impact and compression after impact performance of CFRP. Composites Part A 2002; 33: 483-493.

[8] Caprino G. and Lopresto V. On the penetration energy for fibre-reinforced plastics under low-velocity impact conditions. Composite Science and Technology 2001; 61: 65-73.

[9] Hirei Y., Hamada H. and Kim J.K. Impact response of woven glass-fabric composites – I. Effect of fibre surface treatment. Composite Science and Technology 1998; 58: 91-104.

[10] Abrate S. Modelling of impacts on composite structures. Composite Structures 2001; 51: 129-138.

[11] Christoforou A.P. Impact dynamics and damage in composite structures. Composite Structures 2001; 52: 181-188.

[12] Sutherland L.S. and Guedes Soares C. The effects of test parameters on the impact response of glass reinforced plastic using an experimental design approach. Composites Science and Technology 2002; 63: 1-18

[13] Sutherland L.S. and Guedes Soares C. Impact Behaviour of Low Fibre-Volume, Woven Roving E-Glass / Polyester Laminates. Submitted to Composites Science and Technology 2002.

[14] Shivakumar K.N., Elber W. and Illg W. Prediction of impact force and duration due to low-velocity impact on circular composite laminates. J. Appl. Mech. 1985;52:674-680.